

PATHWAYS AND MECHANISMS FOR THERMOLYSES OF METHYLATED ACENES

P.S. Virk and V.J. Vlastnik
Department of Chemical Engineering
M. I. T., Cambridge, MA 02139

KEYWORDS: Thermolysis, Reaction Paths, Kinetics, Demethylation, Hydrogen Transfer.

ABSTRACT: Thermolyses of three methylated aromatic acenes, 9,10-Dimethyl-Anthracene (910DMA), 9-Methyl-Anthracene (9MA), and 1,4-Dimethyl-Naphthalene (14DMN), were studied to mimic the thermal decomposition of methyl-substituted aromatic moieties in coal and coal liquids. Experiments were conducted at temperatures from 315-550 C, initial substrate concentrations from 0.08-2.5 mol/l, and fractional substrate conversions, X, from 0.05-0.99. The observed thermolysis kinetics ranged from ~3/2 to 2 order wrt substrate, with activation energies ~45 kcal/mol. At fixed T = 370 C and [C]₀ ~0.85 mol/l, decomposition half-lives for (910DMA, 9MA, 14DMN) were respectively (9900, 23000, 530000) s. In general, three primary pathways operated during thermolysis of these methylated acenes. For 910DMA these were: (P1) Hydrogenation, to 9,10-Dihydro-9,10-Dimethyl-Anthracene, (P2) Demethylation, to 9-Methyl-Anthracene, and (P3) Methylation, to 1,9,10-Trimethyl-Anthracene (and isomers). These pathways further operate upon the primary products themselves, forming 9,10-Dihydro-9-Methyl-Anthracene, a host of Dimethyl-Anthracenes (1,9-, 1,10-, 2,9-, and 3,9-isomers), and Anthracene, as well as 1- and 2-Methyl-Anthracenes. Observed initial selectivities to the primary hydrogenation, demethylation, and methylation products were respectively about 0.1, 0.3 and 0.1, while the selectivities to methane gas and to heavy products were respectively 0.2 and 0.2. A radical mechanism comprising 10 elementary steps was proposed for 910DMA thermolysis at low conversions, and shown to account for the experimental observations.

INTRODUCTION

Motivation. The present work on thermolysis of methylated aromatic acenes is part of a continuing study [1,2] of simple substrates that mimic the chemical moieties-found in complex fossil materials of engineering interest. The 910DMA, 9MA and 14DMN substrates were chosen because their acene rings are prototypical of the aromatic ring systems found in fossil materials, while their methyl groups model the electron-donating substituents commonly pendant thereon.

Previous Work. Neither 910DMA nor 14DMN thermolyses appear to have been studied previously. The literature contains two earlier references to 9MA thermolysis [3, 4].

Outline. We first describe the experiments and present results for the concentration histories, product selectivities, and kinetics observed during 910DMA thermolysis. These results are combined with data from 9MA and 14DMN thermolyses to provide general reaction pathways for the decomposition of multiply-methylated acenes. Finally, a radical mechanism comprising 10 elementary steps is proposed for 910DMA thermolysis at low conversions, and shown to accommodate many of the experimental observations.

EXPERIMENTAL

Conditions. The upper portion of Table 1 summarizes conditions for the experiments, listing the model substrates, their structures and the ranges of temperatures, holding times and initial concentrations studied, as well as the temperatures at which light gases were analysed. Thermolyses were conducted in batch reactors, volume 0.6 ml, made from 1/4" stainless steel Swagelok parts. The reactors were charged with weighed amounts of biphenyl (internal standard) and substrate (say, 910DMA) totalling 0.30 g, sealed and placed in an isothermal, fluidized-sand bath for the appropriate holding times, after which they were quenched in ice-water, and their contents extracted into methylene chloride. Reactor contents were in the liquid phase during all experiments.

Assays. Gaseous and liquid thermolysis products were identified and analyzed by GC, augmented by GC/MS. All gas peaks were identified by injections of standards. Most liquid products were identified by injections of standards with some minor liquid products identified by determining their masses by GC/MS and relating their retention times to those of known molecules. Heavy thermolysis products, mostly dehydrogenated dimers of the substrates, were identified by GC/MS. For example, in 910DMA thermolyses, the MS of a prominent late GC peak showed a molecular ion at mass 410 and a fragment at mass 205, suggestive of a bibenzyl, dehydrogenated dimer of 910DMA. Product assay trains developed for each substrate using the preceding GC and GC/MS techniques typically identified ~15 reaction products. Identified products accounted for > 90% of the reacted mass at low substrate conversion, X < 0.4, and > 65% of the reacted mass at the highest conversions, X > 0.8. Experimental details are available [5].

RESULTS and DISCUSSION

Histories. Fig. 1 chronicles the concentration histories of substrate and products during thermolysis of 910DMA at T = 370 C and [C]₀ = 0.82 mol/l, using arithmetic coordinates of absolute mols J of either substrate or product present in the reactor versus reaction holding time t in seconds. Part (a), left panel, shows that the substrate 910DMA decayed monotonically, with half-life t* ~ 9000 s. The major products formed, in order of initial abundance, were 9MA, methane, abbr CH₄, various trimethyl-anthracenes, abbr TMA, dihydro-dimethyl-anthracenes, abbr DHDMA, and anthracene, abbr ANT. The main product 9MA exhibited a maximum, characteristic of an intermediate in the demethylation sequence 910DMA → 9MA →

ANT. The formation of TMA and DHDMA products concurrent with 9MA shows that during 910DMA thermolysis, methylation and hydrogenation always occur in parallel with demethylation. Part (b), right panel, shows minor product histories, including those of the dimethyl-anthracene isomers, 1,9-, 1,10-, 2,9-, and 3,9-DMA, all of which arose subsequent to 9MA, the methyl-anthracene isomers, 1MA and 2MA, both of which arose subsequent to ANT, and the 9,10 dihydro- hydrogenated species, DHMA and DHA, both formed subsequent to their parent aromatic. The foregoing suggest that the minor 1,9-, 1,10-, 2,9-, and 3,9-DMA products originated by methylation of 9MA rather than the isomerization of 910 DMA substrate and also that 1MA and 2MA likely arose from methylation of ANT rather than isomerization of 9MA.

Selectivities. Fig. 2 depicts the preceding product history data as selectivity diagrams, with ordinate of product selectivity $S = \text{mols J produced/mol of substrate 910DMA decomposed}$, and abscissa of substrate fractional conversion X . Part (a), left panel, shows that the products formed at the lowest conversions were 9MA, TMA, and CH₄ with selectivities respectively $S = 0.35, 0.20$ and 0.20 , as well as DHDMA and ANT, with respective $S \sim 0.06$ and 0.03 . With increasing conversion, 9MA selectivity remained roughly constant at $S \sim 0.4$ for $X < 0.80$, while TMA and CH₄ exhibited mirror image selectivity decreases and increases, likely reflecting demethylation of the TMA; the selectivity of DHDMA decreased monotonically, to near zero at the highest conversions, while ANT selectivity increased monotonically, reflecting its position as demethylation terminus. The sum of the selectivities of all identified liquid products (circles) was ~ 0.75 over the major range of conversions, $0.2 < X < 0.8$, from which the selectivity of unidentified, mostly heavy, product formation is inferred to be ~ 0.25 .

Product Ratios. The importance of each of the observed hydrogenation, methylation, and methane formation pathways relative to the dominant demethylation pathway can be assessed from the respective primary product ratios R , namely $R[\text{DHDMA}/9\text{MA}]$, $R[\text{TMA}/9\text{MA}]$ and $R[\text{CH}_4/9\text{MA}]$. Of these, the ratio of hydrogenation to demethylation, $R[\text{DHDMA}/9\text{MA}] \rightarrow 0.4$ at the lowest conversions, $X \rightarrow 0$, and then decreased rapidly to 0.04 ± 0.02 for $X > 0.20$. This variation of $R[\text{DHDMA}/9\text{MA}]$ versus X was essentially independent of initial concentration and temperature, implying that the hydrogenation and demethylation pathways were of similar overall order wrt substrate and possessed similar activation energies. Fig. 3(a), left panel, shows that the ratio of methylation to demethylation, $R[\text{TMA}/9\text{MA}] = 0.24$ for $X > 0.20$ at all temperatures while Fig. 3(b), right panel, shows that the ratio of methane formation to demethylation, $R[\text{CH}_4/9\text{MA}] = 0.63$ for $X > 0.20$ at $T = 355$ and 370 C. The sum $R[\text{TMA}/9\text{MA}] + R[\text{CH}_4/9\text{MA}] \sim 0.87$ was close to unity, accounting for the methyl radicals implicitly associated with the demethylation pathway. It is interesting that $\sim 3/4$ of all methyl radicals formed were quenched by hydrogen abstraction, forming methane gas, while $\sim 1/4$ were trapped by addition to the 910DMA substrate, eventually appearing as TMAs.

Kinetics. Observed decomposition kinetics are illustrated in Fig. 4. Part (a), left panel, is a log-log plot of decay half-life t^* versus initial concentration $[C]_0$ at fixed temperature. The data for 910DMA substrate (circles), spanning two decades of $[C]_0$, describe a line of slope $-1/2$, which implies that the decomposition was of $3/2$ order wrt substrate. Part (b), right panel, is an Arrhenius type of semi-log plot, showing decay half-life t^* versus the reciprocal of a scaled absolute temperature $\Theta = 0.004573^*(T \text{ C} + 273.2)$. Data for 910DMA substrate (circles), spanning two decades of t^* , define a line of slope ~ 43 ; on these coordinates, the slope is directly the activation energy of decomposition E^* , in kcal/mol. Decay half-lives obtained for thermolyses of the other substrates, 9MA (squares) and 14DMN (triangles) are also shown in Fig. 4. Kinetics are summarized in Table 1, in the form of decay half-lives at $T = 370$ C, orders wrt substrate, and Arrhenius parameters ($\log A$, E^*). The relative decomposition rates of 910DMA, 9MA, and 14DMN were roughly in the ratio $1 : \sim 1/2 : \sim 1/50$. All decompositions were of high order, between $3/2$ and 2 , wrt substrate, and exhibited activation energies ~ 45 kcal/mol.

Pathways. The concentration history, selectivity and product ratio observations detailed for 910DMA substrate were broadly echoed in thermolyses of the other two substrates, 9MA and 14DMN, as well. From these results, general decomposition pathways for multiply-methylated acenes containing, say, X total methyl substituents were deduced. Fig. 5 shows that three primary pathways operate in parallel upon the original X -Methyl Acene, namely: (P1) Hydrogenation, to the Dihydro- X -Methyl Acene, (P2) Demethylation, to the $(X-1)$ -Methyl-Acene, and (P3) Methylation, to the $(X+1)$ -Methyl-Acene. Too, the demethylated acene product is associated with formation of methane gas CH₄, and the scheme also includes formation of a heavy bibenzylic dimer of the X -Methyl Acene. Further, the primary demethylation and methylation products in the above scheme can be secondarily operated upon by a pathway triad analogous to the one from which they arose, leading respectively to the formation of $(X-2)$ - and $(X+2)$ -Methyl Acenes, and thence, recursively, to all levels of methylation from the denuded parent to the fully methylated acene nucleus. In 910DMA thermolysis the primary pathway triad is (P1) Hydrogenation, to DHDMA, (P2) Demethylation, to 9MA, and (P3) Methylation, to TMA. Continued operation of this general pathway triad upon the primary products is evidenced by the appearance, at high conversions, of DHMA, a host of DMAs (1,9-, 1,10-, 2,9-, and 3,9-isomers), ANT, and 1MA and 2MA. Pathway results for all substrates are summarized in the bottom sections of Table 2, which show, in generalized form, major product selectivities and ratios at $T = 370$ C and conversions $X = 0.05$ and 0.4 . Results for 9MA were qualitatively similar to those obtained for 910DMA, but showed a two-fold greater selectivity to the methylated product, and also roughly two-fold greater ratios of hydrogenated/demethylated and of methylated/demethylated products at low conversions. Results for 14DMN were noteworthy in that the hydrogenation pathway (P2) was essentially absent, with other product selectivities and ratios akin to those for 910DMA.

Mechanism. A possible mechanism for 910DMA thermolysis is presented in Fig. 6. This elementary step "graph" is constructed with substrate and all stable molecular products arrayed in the bottom row and unstable radical intermediates arrayed in the top row. Reaction "nodes", arrayed in the middle row, connect the individual species in the bottom and top rows with arrows indicating the initial direction of reaction (all reactions are, of course, reversible). Arrow thicknesses are set roughly proportional to elementary reaction traffic, as inferred from the observed product selectivities. Initiation reactions are denoted by solid interconnecting lines, propagation reactions by various kinds of dashed lines and termination reactions by dotted lines. The 910DMA substrate is in the middle of the bottom row, with light (propagation) products to its right and heavy (termination) products, to its left. The free-radical cycle is initiated by the bimolecular disproportionation of substrate (R1), an intermolecular hydrogen transfer reaction, to form the respectively dehydrogenated and hydrogenated radical species 910DMA* and HDMA*. Of these, the latter can either abstract hydrogen from 910DMA by (R2), to form DHDMA products, or undergo a β -scission type of radical decomposition by (R3), forming 9MA product and a methyl radical CH₃*. The CH₃* can either abstract H from 910DMA by (R4), to form methane product, or add to 910DMA by (R5), to form the trimethyl radical HTMA1*. The latter can then abstract H from 910DMA via (R6) to form the observed TMA product. The radical cycle is terminated by the species 910DMA* and HDMA* engaging in both pure- and cross-combinations, (R7-R9), to form various dimeric products. HDMA* radical can also terminate by disproportionation, (R10), to form 910DMA and DHDMA.

The proposed mechanism evidently accounts for most of the major products, 9MA, TMA, DHDMA, CH₄ and heavies, observed during the initial stages of 910DMA thermolysis. Each of the observed triad of primary pathways, namely, P1 hydrogenation, P2 demethylation and P3 methylation, also arise naturally as limiting cases of the elementary step graph, with P1 comprising the set [R1, R2, R7], P2 the set [R1, R3, R4, R7] and P3 the set [R1, R3, R5, R6, R8]. The stoichiometry of these sets restricts the maximum selectivity of each major product to 1/3, which is of the magnitude of the highest selectivities actually observed. The mechanism also offers some theoretical insights. It suggests that the relative kinetics of the observed hydrogenation and demethylation pathways, (P1)/(P2), are essentially controlled by the HDMA* radical, through the ratio of its H-abstraction to β -scission reactions (R2)/(R3). Further, the observed methylation to demethylation pathway ratio, (P3)/(P2), is essentially governed by competition between methyl radical reactions (R4) and (R5), in which CH₃* either abstracts H from or adds to the 910DMA substrate.

In future work it is hoped that the mechanism presented above will provide a basis for both the further quantitative modelling and numerical simulation of 910DMA thermolysis and also for the construction of new, analogous, mechanisms for 9MA and 14DMN thermolyses.

ACKNOWLEDGEMENT: This work was supported by Cabot Corporation, Boston, MA.

REFERENCES

- [1] Virk, P.S.; Vlastnik, V.J.: PREPRINTS, Div. of Petrol. Chem., ACS, 38(2), 422 (1993).
- [2] Virk, P.S.; Vlastnik, V.J.: PREPRINTS, Div. of Fuel Chem., ACS, 37(2), 947 (1992).
- [3] Pomerantz, M.; Combs Jr., G.L.; Fink, R.: J. Org. Chem., 45, 143 (1980).
- [4] Smith, C.M.; Savage, P.E.: A.I.Ch.E. J., 39, 1355 (1993).
- [5] Vlastnik, V.J.: Sc.D. Thesis, Dept. of Chem. Eng., MIT, Cambridge, MA (1993).

Table I. Experimental Grid, Kinetics, and Major Product Selectivities and Ratios for Thermolyses of Methylated Acenes.

Substrate Structure	910DMA	9MA	14DMN	
Experimental Grid				
Temperature, T C	315-409	315-409	370-550	
Holding Time, t s	450-57600	450-57600	150-115200	
Initial Concentration, [C] ₀ , mol/l	0.082-2.47	0.082-2.06	0.081-2.07	
Gas Analyses at T C	335, 370	370	450	
Kinetics				
Decay Half-Life, t* s at T = 370 C	9900	23000	530000	
Order wrt substrate	1.53	1.50	2.05	
Arrhenius Parameters (log A, E*)	(10.6, 43.1)	(11.4, 46.4)	(8.5, 42.0)	
Product Selectivities at T = 370 C	X			
Demethylated	0.4	0.42	0.37	0.32
Methylated	0.4	0.10	0.22	0.10
Hydrogenated	0.05	0.06	0.03	0
Heavies	0.4	0.15	0.13	0.06
Product Ratios at T = 370 C	X			
[Hydrogenated/Demethylated]	0.05	0.21	0.43	0
	0.4	0.04	0.05	0
[Methylated/Demethylated]	0.05	0.35	0.69	0.54
	0.4	0.28	0.36	na

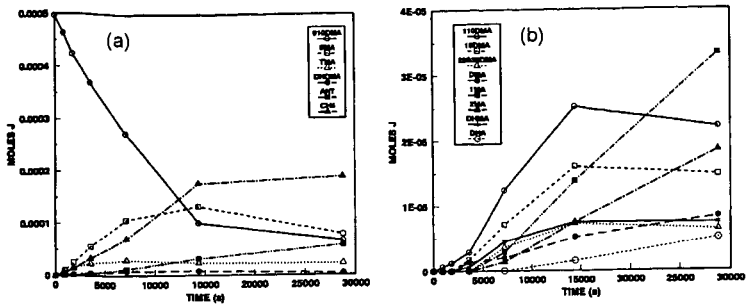


Fig. 1. Concentration Histories in 910DMA Thermolysis at $T = 370\text{ C}$ and $[910DMA]_0 = 0.82\text{ mol/l}$. (a) Major and (b) Minor Products.

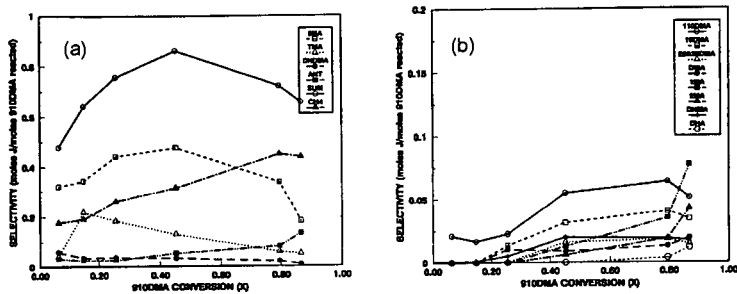


Fig. 2. Product Selectivities in 910DMA Thermolysis at $T = 370\text{ C}$ and $[910DMA]_0 = 0.82\text{ mol/l}$. (a) Major and (b) Minor Products.

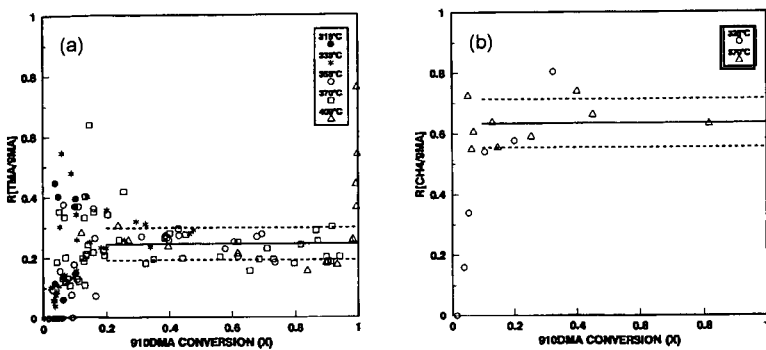


Fig. 3. Major Product Ratios in 910DMA Thermolyses at $T = 315\text{ to }409\text{ C}$ and $[910DMA]_0 = 0.82\text{ mol/l}$. (a) $R[\text{TMA}/9\text{MA}]$ and (b) $R[\text{CH}_4/9\text{MA}]$.

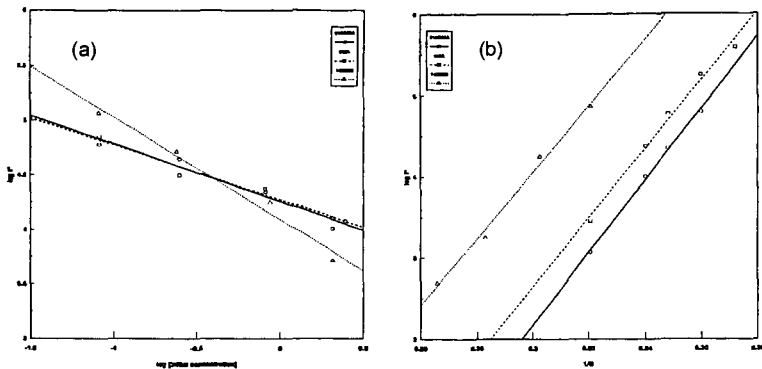


Fig. 4. Decay Half-Lives in Methylated Acene Thermolyses. (a) Effect of Initial Concentration at Fixed $T = 355\text{ C}$ (910DMA), 370 C (9MA), and 450 C (14DMN), and (b) Effect of Temperature at Fixed $[C]_0 \sim 0.85\text{ mol/l}$ (all).

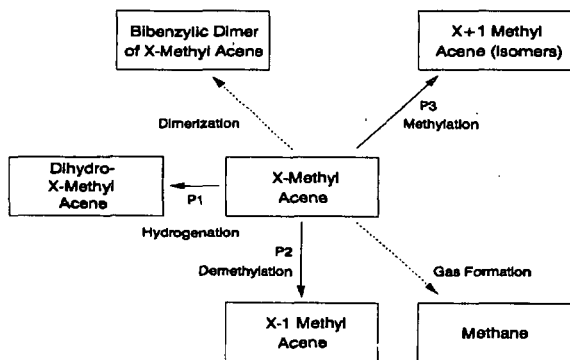


Fig. 5. General Decomposition Pathways for an X-Methyl Acene.

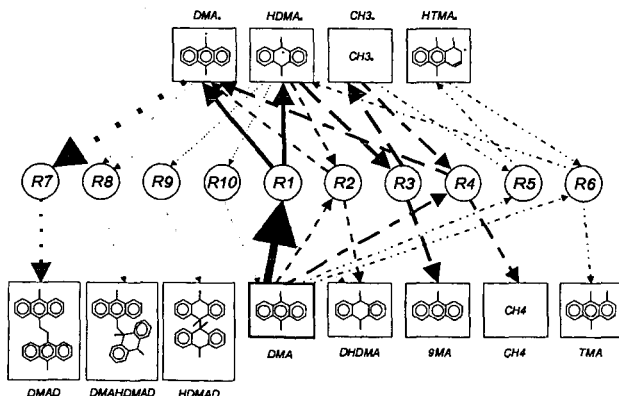


Fig. 6. Elementary Step Graph of 910DMA Thermolysis Mechanism Showing Relative Reaction Traffic at Low Substrate Conversions.